

# Next generation population synthesis of accreting white dwarfs: I. Hybrid calculations using BSE + MESA

Hai-Liang Chen<sup>1,2,3,4\*</sup>, T. E. Woods<sup>4</sup>, L. R. Yungelson<sup>5</sup>, M. Gilfanov<sup>4,6,7</sup>, Zhanwen Han<sup>1,2</sup>

<sup>1</sup>Yunnan Observatories, Chinese Academy of Sciences, Kunming, 650011, China

<sup>2</sup>Key Laboratory for the Structure and Evolution of Celestial Objects, Chinese Academy of Sciences, Kunming 650011, China

<sup>3</sup>University of Chinese Academy of Sciences, Beijing 100049, China

<sup>4</sup>Max Planck Institute for Astrophysics, Karl-Schwarzschild-Str. 1, Garching b. München 85741, Germany

<sup>5</sup>Institute of astronomy, RAS, 48 Pyatnitskaya Str., 119017 Moscow, Russia

<sup>6</sup>Kazan Federal University, Kremlevskaya str.18, 420008, Kazan, Russia

<sup>7</sup>Space Research Institute of Russian Academy of Sciences, Profsoyuznaya 84/32, 117997 Moscow, Russia

16 March 2022

## ABSTRACT

Accreting, nuclear-burning white dwarfs have been deemed to be candidate progenitors of type Ia supernovae, and to account for supersoft X-ray sources, novae, etc. depending on their accretion rates. We have carried out a binary population synthesis study of their populations using two algorithms. In the first, we use the binary population synthesis code BSE as a baseline for the “rapid” approach commonly used in such studies. In the second, we employ a “hybrid” approach, in which we use BSE to generate a population of white dwarfs (WD) with non-degenerate companions on the verge of filling their Roche lobes. We then follow their mass transfer phase using the detailed stellar evolution code MESA. We investigate the evolution of the number of rapidly accreting white dwarfs (RAWDs) and stably nuclear-burning white dwarfs (SNBWDs), and estimate the type Ia supernovae (SNe Ia) rate produced by “single-degenerate” systems (SD). We find significant differences between the two algorithms in the predicted numbers of SNBWDs at early times, and also in the delay time distribution (DTD) of SD SNe Ia. Such differences in the treatment of mass transfer may partially account for differences in the SNe Ia rate and DTD found by different groups. Adopting 100% efficiency for helium burning, the rate of SNe Ia produced by the SD-channel in a Milky-way-like galaxy in our calculations is  $2.0 \times 10^{-4} \text{yr}^{-1}$ , more than an order of magnitude below the observationally inferred value. In agreement with previous studies, our calculated SD DTD is inconsistent with observations.

## Key words:

binaries: close – stars: evolution, population synthesis – supernovae

## 1 INTRODUCTION

Type Ia supernovae (SNe Ia) have been used with great success as standardizable candles, allowing for the measurement of cosmological parameters (Riess et al. 1998; Perlmutter et al. 1999). SNe Ia are also of great importance for galactic chemical evolution (e.g. Matteucci & Greggio 1986). It is widely accepted that they are thermonuclear explosions of carbon-oxygen (CO) white dwarfs (WDs). The compact, degenerate structure of the exploding stars in SNe Ia was recently confirmed by early-time multi-wavelength observations of SN2011fe (Nugent et al. 2011;

Bloom et al. 2012). However, the nature of SNe Ia progenitors is still unclear (see Hillebrandt et al. 2013 for a recent review). The models for the progenitors of SN Ia fall into two categories: the single degenerate (SD) model (Whelan & Iben 1973) and the double degenerate (DD) model (Tutukov & Yungelson 1981; Iben & Tutukov 1984; Webbink 1984). In the standard SD-model a WD accretes matter from a non-degenerate companion, which may be a main-sequence, subgiant, or red giant star. In order to grow, a WD must accumulate mass via nuclear-burning of hydrogen into helium, and helium into carbon and oxygen. When the WD mass reaches  $M_{\text{Ch}}$ , the WD explodes as an SN Ia.

However, theoretical and observational challenges persist for both scenarios. The fundamental difficulty for the SD-model is the narrow range of accretion rates

\* E-mail: chenhl@mpa-garching.mpg.de

( $\sim \text{few} \times 10^{-7} M_{\odot} \text{ yr}^{-1}$ ) for which steady nuclear-burning and efficient accumulation of mass by the WD is possible (Paczynski & Zytkov 1978). This requires specific combinations of donor and accretor masses, restricting the typical delay time between formation of a binary and a SN Ia by  $\sim 1$  Gyr, and similarly the peak production of SNe Ia in this channel within a similar delay time. Another problem is the treatment of the excess matter which cannot be processed through steady nuclear-burning. This is typically *assumed* either to form an extended envelope around the WD, leading to the formation of a common envelope, or to be lost from the system in the form of an optically thick wind.

Therefore, the viability of the SD-scenario depends critically on the treatment of mass transfer and resulting accretion rate, which defines whether the WD may, presumably grow in mass. White dwarfs with different accretion rates are associated with different sources and phenomena, e.g. supersoft X-ray sources (SSSs) and novae. Comparing observations with the number of SSSs and the nova rate predicted by population synthesis models can be used to verify calculations, and also to constrain the SD-channel.

Because of the relatively high mass transfer rates needed to sustain steady nuclear burning, these sources are almost always associated with mass transfer on the donor’s thermal timescale (thermal timescale mass transfer, TTMT). In binary population synthesis codes, TTMT is typically accounted for using a simple analytic treatment. However, such analysis typically assumes implicitly that the donor star remains in *thermal equilibrium*, with the entire star (or at least its entire envelope) responding at once, despite mass transfer being driven by the *thermal disequilibrium* of the donor (e.g. Yungelson et al. 1995; Ruiter, Belczynski & Fryer 2009; Bours, Toonen & Nelemans 2013). This is particularly important in treating mass loss from red giants – detailed calculations reveal that the rapid expansion of the donor envelope in response to mass transfer, expected in the simplified treatment of adiabatic models (Hjellming & Webbink 1987), does not necessarily occur (Woods & Ivanova 2011). This is critical in determining the circumstances under which a binary will undergo a common envelope (CE) phase. In those cases where the binary will undergo a CE regardless, it is also possible that some mass may be accreted prior to this phase, and any accreting WD may appear briefly as an SSS. This is unaccounted for in the traditional treatment of mass transfer in population synthesis.

In this paper (Paper I), we investigate in detail mass transfer in the semidetached systems with nuclear-burning WD (NBWD) accretors and main-sequence, Hertzsprung gap and red-giant donors. We pay special attention to the systems in which WDs burn hydrogen steadily (SNBWDs) and to the systems with accretion rates exceeding the upper limit for steady burning, but too low for the formation of a common envelope, (“rapidly accreting white dwarfs” (RAWDs), Lepo & van Kerkwijk 2013)<sup>1</sup>. For this, we produce a grid of  $\sim 3 \times 10^4$  evolutionary sequences of close

binary models with different initial combinations of WD accretors and nondegenerate donors, and with differing orbital periods at the onset of Roche lobe overflow, calculated by the detailed stellar evolutionary code MESA (Paxton et al. 2011, 2013). Our models are compared with the ones obtained using analytic descriptions of mass-transfer. In order to relate our work to observations, we compare the predicted evolution of the numbers of SNBWD, RAWD, and the rates of SNe Ia given two star formation histories: an instantaneous burst of star formation, and a constant star formation rate for 10 Gyr, approximating early and late type galaxies respectively. In a subsequent paper (hereafter Paper II), we will incorporate spectral models for nuclear-burning white dwarfs. This will allow us to more meaningfully test the predictions of our model.

We describe the method of calculations in §2, highlight the effect of varying treatments of TTMT in §3, follow with a discussion of how some observables vary with changing MT treatment in §4, in particular the predicted populations of RAWDs, SNBWDs, and SNe Ia. Summary and conclusions are presented in §5.

## 2 THE METHOD OF CALCULATIONS

### 2.1 Mass loss treatment in binary population synthesis

The method applied to study different populations of binary stars and the products of their evolution is binary population synthesis (BPS). In population synthesis, one convolves the statistical data on initial parameters and birthrates of binaries with scenarios for their evolution. This allows one to study birthrates and numbers of binaries of different classes and their distributions over observable parameters.

There are two basic algorithms applied to study semidetached stages of evolution in BPS codes. The “rapid” one employs analytic formulae, approximating each evolutionary phase using simple fits from detailed calculations. Mass transfer is accounted for by calculating the radial response of the donor star and its Roche radius. Alternatively, one may employ a “hybrid” approach which entails two steps. Relevant to our present study, first we obtain the population of WD binaries with nondegenerate donors at the onset of mass transfer by means of a BPS code. Here we use the publicly available code BSE<sup>2</sup> (Hurley, Tout & Pols 2002), which we have modified slightly (see below). In the second step, in order to obtain an accurate description of post-RLOF mass-loss rates, we compute the mass transfer rate and response of the donors in this population by drawing from a grid of  $3 \times 10^4$  evolutionary sequences of models for WDs with MS, HG or FGB companions computed by MESA (Paxton et al. 2011, 2013), in practice, using about  $\sim 4000$  such tracks. The advantage of this approach is the possibility to describe  $\dot{M}$  accounting for the response of the donor. This also allows one to avoid the exclusion of any short evolutionary stages.

It is known from the earliest studies of close interacting binaries (see, e.g. Morton 1960; Paczyński, Ziolkowski & Zytkov 1969; Paczyński & Sienkiewicz 1972) that, depending on the

<sup>1</sup> It was shown by Paczyński (1971) that putting a  $\sim 10^{-3} M_{\odot}$  hydrogen-helium envelope atop a hot ( $\log T_e = 5.0$ ) carbon-oxygen WD transforms it into a red giant ( $\log T_e = 3.6$ ); this may be avoided, if excess of the matter is removed by postulated optically-thick stellar wind (Hachisu, Kato & Nomoto 1999).

<sup>2</sup> <http://astronomy.swin.edu.au/~jhurley/bsedload.html>

evolutionary status of the Roche-lobe-overflowing star (the donor) and the mass ratio of the components, the donor may lose mass on a timescale defined by the dynamical, thermal, or nuclear evolution of the donor, or the loss of angular momentum. In practice, this means that the mass-loss rate depends on relations between the response of the Roche lobe radius to mass loss  $\zeta_{RL} \equiv \left(\frac{\partial \ln R_{RL}}{\partial \ln M_1}\right)$ , the adiabatic hydrostatic response of the stellar radius  $\zeta_{ad} \equiv \left(\frac{\partial \ln R}{\partial \ln M_1}\right)_{ad}$ , the thermal-equilibrium response of the same  $\zeta_{th} \equiv \left(\frac{\partial \ln R}{\partial \ln M_1}\right)_{th}$ , the nuclear evolution of the radius, and finally the angular momentum loss timescale. If  $\zeta_{ad} > \zeta_{RL} > \zeta_{th}$ , the star remains in hydrostatic equilibrium, but does not remain in thermal equilibrium; in this case mass loss occurs on the thermal timescale of the star. If  $\zeta_{RL} > \zeta_{ad}$ , the star cannot remain in hydrostatic equilibrium, and mass loss proceeds on the dynamical timescale. If  $\zeta_{ad}, \zeta_{th} > \zeta_{RL}$ , mass loss occurs due to the expansion of the star during its evolution on the nuclear timescale, or due to the shrinkage of the Roche lobe owed to angular momentum losses.

Dynamical or thermal timescale mass loss is common for initial stages of mass exchange. In “rapid” BPS codes it is assumed that, if RLOF leads to dynamical mass loss (according to some assumed criteria), then the formation of a common envelope is unavoidable. In this case, no further computations of the mass transfer rate or the response of the donor star are carried out. Mass loss is assumed to occur on the thermal timescale if, after removal of an infinitesimally small amount of mass, the radius of the star in thermal equilibrium is predicted to be larger than the (volume-averaged) Roche lobe radius. In the simplest formulation, the mass loss rate is approximated as

$$\dot{M}_{th} = M/\tau, \quad (1)$$

where  $M$  is the mass of the Roche-lobe filling star and  $\tau$  is an estimate of the thermal timescale. In general, the definition of  $\dot{M}_{th}$  is not unique and differs between codes because of our present lack of understanding of what fraction of the star is involved in mass exchange (i.e. to what depth do we evaluate  $\tau_{th}$ ?). Then, typically, one writes  $\dot{M}_{th} = k \cdot R_d L_d / GM'$ , where, in the simplest cases,  $k \sim 1$ ,  $M'$  is the instantaneous total mass of the star or the mass of the stellar envelope. In slightly more sophisticated cases,  $k$  may be a function of the mass-radius response functions of the donor and its Roche radius (e.g. Ivanova & Taam 2004). Moreover, for  $R_d$  and  $L_d$  the values corresponding to stars in **thermal equilibrium** are usually taken, despite mass transfer being driven by the **thermal disequilibrium** of the donor star. As a result, just after RLOF  $\dot{M}$  is constant or slowly declining as  $M_d$  falls (see Fig. 2 below). However, Langer et al. (2000) (see also Podsiadlowski et al. 2002) clearly showed that equations similar to Eq. (1) provide only the order of magnitude of the mass transfer rate.

Although detailed calculations accounting for the response of the donor are preferable, the use of the “hybrid” technique has so far been limited by the available computing power. If too crude a grid of evolutionary models is used, it may result in spurious effects. Only recently, with the advent of the rapid and robust stellar evolutionary code MESA, has it become possible to increase the number of sufficiently detailed tracks by an order of magnitude, to several 10,000,

which can be used to adequately describe the evolution of a parental population of  $\sim 100,000$  systems.

Earlier, grids of detailed evolutionary tracks leading to the systems or events of desired type were combined with detailed BPS codes, e.g., by Pfahl et al. (2003) for low and intermediate mass X-ray binaries, Han & Podsiadlowski (2004) for SNe Ia in semidetached systems, Madhusudhan et al. (2008) for ultraluminous X-ray sources. Advantages of this method were recently discussed by Nelson (2012). In this paper, we present the first attempt to use grids of tracks computed by MESA to investigate accreting WDs.

## 2.2 Binary population synthesis for NBWDs

In this paper, we employ both the “hybrid” approach and the “rapid” approach described above. In either case, each evolutionary track for every binary must be scaled by a relative “weight” which accounts for the total number of binaries the track represents. To evaluate the relative “weight” of a binary, we take the IMF of primaries from Kroupa (2001) with lower and upper mass cutoffs  $m_L = 0.1 M_\odot$  and  $m_U = 100 M_\odot$ . We adopt a flat mass ratio distribution (Kraicheva et al. 1979). Binary separations in the range between  $10 R_\odot$  and  $10^6 R_\odot$  are drawn from a flat distribution in logarithmic space (Abt 1983). We assume 50% binarity, i.e.,  $2/3$  of stars are components of binary systems (Duquennoy & Mayor 1991).

Using the latest version of BSE, we computed the evolution of binaries for a regular grid of stars with primary masses varying from  $0.9 M_\odot$  to  $12 M_\odot$  in logarithmic steps of 0.0125, mass ratio of components between 0 and 1 in steps of  $\Delta q = 0.0125$ , and separations of components from  $10 R_\odot$  to  $10^4 R_\odot$  in logarithmic steps of 0.025. Altogether, this gives us a grid of 864,000 systems. As a subset of this grid, we obtain the total population of WD binaries with nondegenerate donors at the onset of mass transfer.

The WD masses at the onset of mass transfer range from  $0.50 M_\odot$  to  $1.40 M_\odot$  and companion masses – from  $0.8 M_\odot$  to  $20 M_\odot$  (see Fig. 1), which are consistent with other binary population synthesis studies (see Fig 3. and 4. in Toonen et al. 2014). For the systems with primary masses or donor masses  $\leq 1.4 M_\odot$  we replaced the original BSE implementation of magnetic braking by the prescription suggested by Rappaport, Verbunt & Joss (1983, Eq. (34) with  $\gamma = 3$ ); this is identical to the magnetic braking law implemented in MESA.

To describe common envelope evolution, we use the prescription suggested by Webbink (1984), with the inclusion of the “binding energy parameter” (de Kool 1990):

$$\alpha_{ce} \left( \frac{G m_{d,f} m_a}{2 a_f} - \frac{G m_{d,i} m_a}{2 a_i} \right) = \frac{G m_{d,i} m_{d,e}}{\lambda R_{d,r}}. \quad (2)$$

Here  $m_{d,i}$  and  $m_{d,f}$  are initial and final donor mass, respectively,  $m_{d,e}$  is the donor envelope mass,  $m_a$  is the accretor mass,  $a_i$  and  $a_f$  are the initial and final binary separations,  $R_{d,r}$  is the Roche lobe radius of the donor at the onset of mass transfer,  $\alpha_{ce}$  is the fraction of the orbital energy used to eject the common envelope and  $\lambda$  is a parameter which characterizes the binding energy of the donor’s envelope. The long-standing problem of the formalism given by

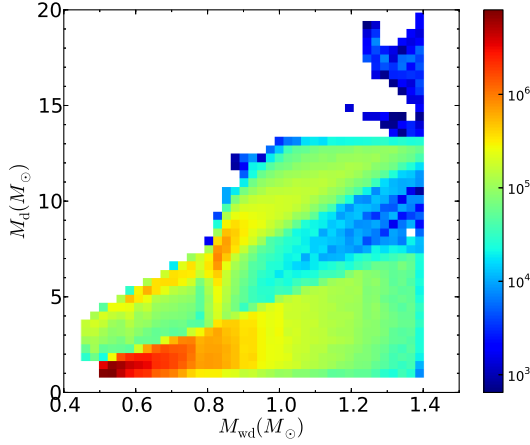


**Figure 1.** WD and donor masses distribution for the population of WD+(nondegenerate companion) binaries with different orbital periods at the onset of mass transfer for a  $10^{11} M_{\odot}$  galaxy in the model B1+M (see table 2).

Eq. (2) is that  $a_f/a_i$  depends on the product of  $\alpha_{ce} \times \lambda$  and these two still uncertain parameters cannot be separated (see Ivanova et al. 2013, for the latest detailed discussion). It is evident that  $\lambda$  should not be constant along the evolutionary track of a star (e.g. Dewi & Tauris 2000). It remains uncertain whether a fraction of the binding energy of the donor may contribute to expelling the envelope and whether there are any other sources contributing to this process.

Davis, Kolb & Willems (2010) computed  $\lambda$ 's for 1 - 8  $M_{\odot}$  AGB stars with varying radii, postulating that the core-envelope interface is located at the position within the star with hydrogen abundance  $X_c = 0.1$ . Then they found that, assuming  $\alpha_{CE} > 0.1$ , it is possible to account for the population of post common envelope binaries found by the SDSS. A similar approach led Zorotovic et al. (2010) to constrain the common envelope efficiency to  $0.2 < \alpha_{CE} < 0.3^3$  Ricker & Taam (2012), based on results of 3D hydrodynamical calculations, limited  $\alpha_{CE}$  from above by 0.4 - 0.5.

Having these uncertainties in mind, we produced a set of WD+(nondegenerate companion) models using BSE, with all CE events following Eq. (2) assuming a constant  $\alpha_{ce} \times \lambda = 0.25$ . In another set of computations, we used fitting formulae for  $\lambda$  (Loveridge, van der Sluys & Kalogera 2011) and  $\alpha_{ce} = 0.25$ .

In the MESA grid, WD masses range from  $0.5 M_{\odot}$  to  $1.3 M_{\odot}$  with an interval of  $0.1 M_{\odot}$ , with an additional final step at  $1.35 M_{\odot}$ . The donor masses range from  $0.9 M_{\odot}$  to  $2.5 M_{\odot}$  with an interval of  $0.025 M_{\odot}$ , with an interval of  $0.1 M_{\odot}$  from  $2.6 M_{\odot}$  to  $3.5 M_{\odot}$ , with an interval of  $0.50 M_{\odot}$  from  $4.0 M_{\odot}$  to  $10.0 M_{\odot}$ , and with an interval of  $1.0 M_{\odot}$  from  $10.0 M_{\odot}$  to  $15 M_{\odot}$ . Initial orbital periods  $\log(P_{orb}/\text{day})$  cover the range from  $-0.3$  to  $2.9$  with a logarithmic step of  $0.1$ . If the parameters of a binary produced in the first step are out of this grid, we computed it individually. In the second step, for every binary we choose the nearest track in

grid of MESA calculations in order to follow the evolution of the system.

The tracks are computed for typical Population I composition with initial hydrogen abundance  $X = 0.70$ , helium abundance  $Y = 0.28$  and metallicity  $Z = 0.02$ .

The retention efficiency of matter accumulated by WDs was estimated on the basis of several ‘‘critical’’ accretion rates. Accreted hydrogen burns stably if  $\dot{M}_{cr} \leq \dot{M}_a \leq \dot{M}_{max}$ , where, we employ the following approximations to the results of Iben & Tutukov (1989)

$$\log(\dot{M}_{max}) \approx -4.6 \times M_{WD}^4 + 17.9 \times M_{WD}^3 - 26.0 \times M_{WD}^2 + 17.5 \times M_{WD} - 11.1, \quad (3)$$

$$\log(\dot{M}_{cr}) \approx -1.4 \times M_{WD}^2 + 4.1 \times M_{WD} - 9.3. \quad (4)$$

Masses are in units of  $M_{\odot}$  and rates in units of  $M_{\odot} \text{ yr}^{-1}$ . For  $\dot{M}_a > 10^{-4} M_{\odot} \text{ yr}^{-1}$ , an optically thick wind can not be sustained (Hachisu, Kato & Nomoto 1999) and a CE is formed. If  $\dot{M}_{max} < \dot{M}_a \leq 10^{-4} M_{\odot} \text{ yr}^{-1}$ , the excess of unburned matter is isotropically reemitted from the system by an optically thick wind. If  $\dot{M}_{cr} > \dot{M}_a \geq 10^{-8} M_{\odot} \text{ yr}^{-1}$ , H burns in mild flashes. Below  $10^{-8} M_{\odot} \text{ yr}^{-1}$  burning flashes are strong and may even erode the dwarf. We apply in this regime a fitting formula for the mass retention efficiency  $\eta_H$  based on the results of Prialnik & Kovetz (1995) and Yaron et al. (2005):

$$\eta_H = -0.075 \times (\log(\dot{M}_a))^2 - 1.21 \times \log(\dot{M}_a) - 4.95. \quad (5)$$

Note,  $\eta_H$  is based on the results for WD temperature  $T_{WD} = 3 \times 10^7 \text{ K}$ . We neglect weak dependence of  $\eta_H$  on WD mass.

To summarize (rates are in  $M_{\odot} \text{ yr}^{-1}$ ):

$$\eta_H = \begin{cases} \text{CE} & \dot{M}_a > 10^{-4} \\ \dot{M}_{max}/\dot{M}_a & \dot{M}_{max} < \dot{M}_a \leq 10^{-4} \\ 1.0 & \dot{M}_{cr} \leq \dot{M}_a \leq \dot{M}_{max} \\ \text{linear interpolation} & \\ \text{between 1 and Eq. (5)} & 10^{-8} < \dot{M}_a < \dot{M}_{cr} \\ \text{Eq. (5)} & 10^{-12} \leq \dot{M}_a \leq 10^{-8}. \end{cases} \quad (6)$$

The ranges of WD masses and accretion rates of steady or unsteady burning regimes of H and He are not identical (see, e.g., Iben & Tutukov 1989). For this reason, in population synthesis studies retention efficiency of He,  $\eta_{He}$ , is considered as a function of  $M_{WD}$  and the rate of H-accumulation. Then, total mass accumulation efficiency is taken as  $\eta_H \times \eta_{He}$ . The value of  $\eta_{He}$  is especially uncertain (Bours, Toonen & Nelemans 2013; Idan, Shaviv & Shaviv 2013; Newsham et al. 2013; Wolf et al. 2013). We assumed, for simplicity,  $\eta_{He} = 1$ . This provides a strict upper limit on the SNe Ia rate.

In the ‘‘rapid’’ approach, the following mass-ratio based criteria for the formation of a CE were applied:  $q = 3$  for MS donors,  $q = 4$  for HG donors. These values are supported by detailed binary evolution studies (Han & Podsiadlowski 2004; Wang, Li & Han 2010). If the donor stars are on the FGB and AGB, we use the prescription of Hjellming & Webbink (1987), despite the fact that this underestimates the stability of mass transferring red giants (Woods & Ivanova 2011), for lack of an alternative prescription. A summary of the NBWDs population models computed in this paper is presented in Table 1. The use of

<sup>3</sup> Note, their sample of post-CE binaries consisted of WD with M-type main-sequence companions. For more massive companions the energetics of the CE phase may differ, see the quoted paper and Zorotovic et al. (2014).

**Table 1.** Computed models

model	$\lambda$	$\alpha$	code
B1	fit <sup>a</sup>	0.25	BSE only
B1+M	fit <sup>a</sup>	0.25	BSE + MESA
B2	$\alpha \times \lambda = 0.25$		BSE only
B2+M	$\alpha \times \lambda = 0.25$		BSE + MESA

<sup>a</sup> The fitting formula from Loveridge, van der Sluys & Kalogera (2011) for  $Z = Z_{\odot}$ .

four different models allow us to compare our results for differing treatment of the second mass transfer phase (analytic or MESA) with that of our choice in CE parameterization (fixed  $\alpha\lambda$ , or an analytic fit of  $\lambda$  from detailed evolutionary calculations with fixed  $\alpha$ ).

### 3 COMPARISON OF MASS TRANSFER TREATMENTS

Here we present examples of computations using two simplified prescriptions for mass transfer and compare them with the results of our detailed stellar evolution calculations using MESA. First, we apply the prescription used in BSE. In solar units, the “thermal timescale” mass transfer rate is defined as  $10^{-7} M_{d,0} RL/M' M_{\odot} \text{ yr}^{-1}$ , where  $M' = M_d - M_c$ ,  $M_c$  is the mass of stellar core. This mass transfer rate is compared to the “nuclear timescale” mass transfer rate given by an *ad hoc* formula  $\dot{M} = 3 \times 10^{-6} [\min(M_d, 5.0)]^2 [\ln(R/R_{RL})]^3 M_{\odot} \text{ yr}^{-1}$ . Then, the minimum of two values for  $\dot{M}$  is chosen. In the illustrative cases presented below,  $\dot{M}$  corresponds to the first of these two formulae.

As the second prescription, we use the formulation applied in the code IBiS (e. g. Yungelson & Livio 1998). If  $\zeta_{th} < \zeta_{RL}$ ,  $\dot{M} = 3.15 \times 10^{-7} RL/M_d^2 M_{\odot} \text{ yr}^{-1}$ . Otherwise, if mass transfer is thermally stable,  $\dot{M}$  is defined by the timescale of growth of the degenerate He-core of the donor. The stabilizing effect of an optically thick wind of from the WD is taken into account in the high- $\dot{M}$  regime.

Finally, in the detailed stellar evolutionary code MESA,  $\dot{M}$  is computed as a stationary subsonic isothermal flow through the vicinity of  $L_1$ , with an additional assumption that  $(R - R_{RL})/H_p \approx 1$ , following Ritter (1988). Here  $H_p$  is the pressure scale height.

In Fig. 2, we show example tracks for three cases of binary evolution, where in each case we have either used one of the two simplified algorithms described above, or MESA. In the upper and middle rows of Fig. 2, the initial white dwarf mass is  $M_{WD} = 0.80 M_{\odot}$ , the initial donor mass is  $M_d = 2.2 M_{\odot}$ , and the initial orbital periods are  $P_{orb} = 0.80$  (upper) & 2.20 days (middle row). In the lower set of panels,  $M_{WD} = 0.80 M_{\odot}$ ,  $M_d = 1.00 M_{\odot}$ ,  $P_{orb} = 3.0$  days. In these three cases, the binaries begin mass transfer on the MS, HG and FGB, respectively. In the initial stage of mass transfer in all three systems  $\zeta_{th} < \zeta_{RL}$  and mass transfer should proceed on thermal timescale. These binaries should not be considered representative of the total population; rather, we

aim here to represent those systems in which a WD reaches  $M_{Ch}$ . Note in particular that WD binaries in which the companion overflows its Roche lobe on the late main-sequence or Hertzsprung gap constitute the overwhelming majority of “successful” progenitors of SNe Ia in all sets of our calculations.

Note that the binary illustrated in the lower row of Fig. 2 would, upon overflowing its Roche lobe on the RGB, form a CE if the Hjellming & Webbink (1987) criterion for stability of mass-transfer were applied (for the purposes of comparison we ignore this criterion here). Although this criterion is widely used, it may overestimate the number of systems which undergo unstable mass-transfer (Woods & Ivanova 2011; Passy, Herwig & Paxton 2012). In the RG case, the binary has short thermal timescale mass transfer phases in the IBiS and MESA-based calculations. Apparently, the formal choice of lower mass transfer mass rate in BSE, ignores existence of TTMT-stage in this case.

In table 2, we present the duration of the RAWD and SNBWD phases, as well as the mass lost by the donor, and the mass accreted in each phase, for each example.

It is worth noting that, with different mass transfer prescriptions, the mass accreted by the WD and the duration of the RAWD and SNBWD phases in different codes are quite different. Compared to the detailed stellar evolution calculations, BSE usually overestimates the duration of the SNBWD phase and underestimates the RAWD phase. The IBiS code underestimates both of them in the MS and HG donor cases. In the MS and HG cases, the amounts of mass accreted during RAWD phase are comparable in BSE and MESA calculations, while they are an order of magnitude smaller in IBiS calculations. In the RG case,  $\Delta M_{WD}$  during the RAWD phase is comparable in IBiS calculations and in MESA calculations. In addition, in all three cases, the amount of mass accreted during the RAWD phase is larger than that in the SNBWD phase. This points again to the need for a proper understanding of accretion at rates exceeding  $\dot{M}_{max}$ . The primary reason for the difference between IBiS calculations and BSE or MESA calculations is that the duration of the phase of effective mass-accumulation ( $\dot{M}_a > \dot{M}_{cr}$ ) in IBiS is about one order of magnitude smaller than that in BSE and MESA.

The difference between IBiS and BSE calculations is partially due to the fact that approximations for  $\dot{M}$  in IBiS are based on results of calculations for binary stars, while in BSE approximations are based on computations for single stars. Both of them produce results different from those, obtained using MESA. Evidently, the difference in mass transfer rate behaviour has an important impact on the results of binary population synthesis for NBWDs. Below, we will show this by using different BPS algorithms.

## 4 RESULTS AND DISCUSSION

### 4.1 Population synthesis of accreting WDs

We model two cases of star formation:

- (I) A starburst — stellar population with mass  $M_t = 10^{11} M_{\odot}$  is formed at  $t = 0$ .
- (II) Constant star formation rate — a galaxy has a constant star formation rate of  $1 M_{\odot}/\text{yr}$  for 10 Gyr.

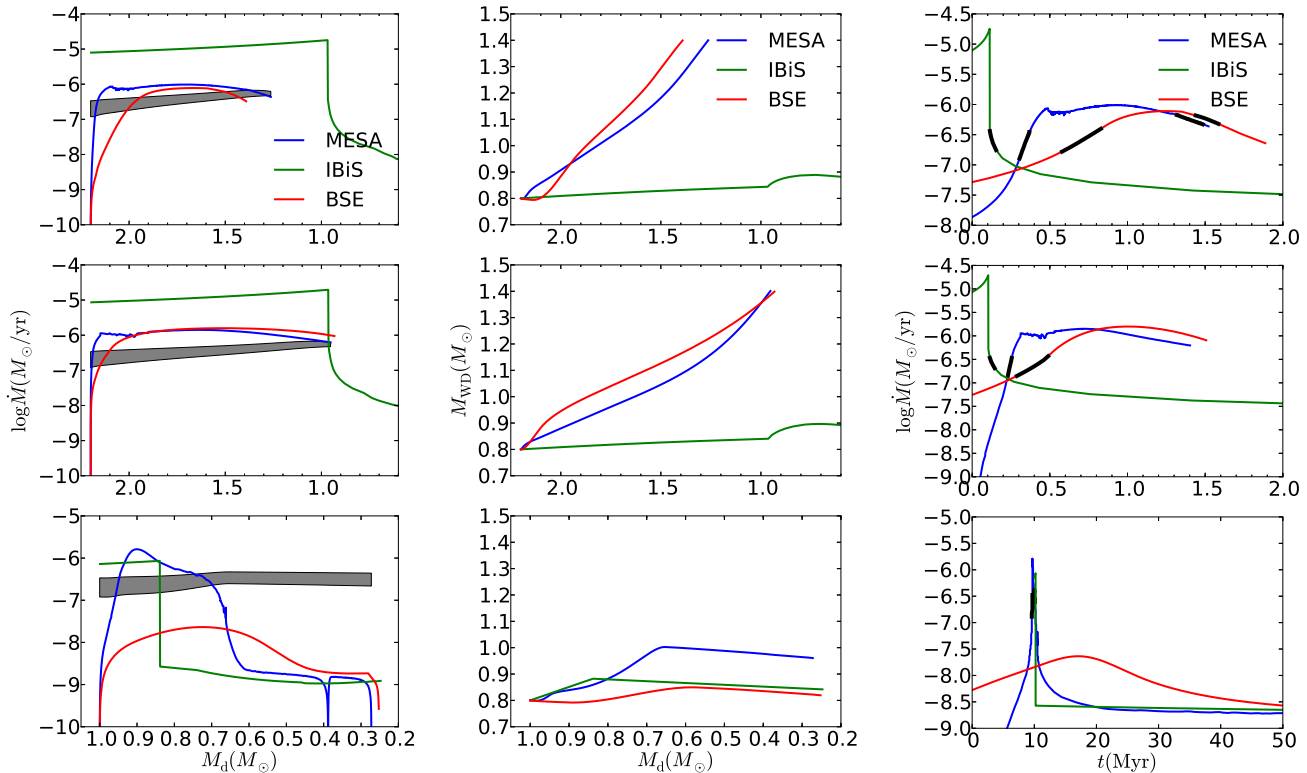


**Figure 2.** Comparison of the evolution of mass transfer rate and mass of the accretor as a function of donor mass (left and middle panels). The right set shows the dependence of  $\dot{M}$  on time. At the onset of mass transfer  $M_{\text{WD}} = 0.80 M_{\odot}$ ,  $M_{\text{d}} = 2.20 M_{\odot}$ ,  $P_{\text{orb}} = 0.80$ , 2.0 days in the upper and middle panels, respectively. In the lower panel, the binary parameters are  $M_{\text{WD}} = 0.8 M_{\odot}$ ,  $M_{\text{d}} = 1.00 M_{\odot}$ ,  $P_{\text{orb}} = 3.0$  days. For these three binaries, mass transfer begins on the MS, HG and RG branch, respectively. In the right set, the thick black line shows the time spent in the stable burning regime.

**Table 2.** Comparison of the duration of RAWD and SNBWD phases, accreted mass  $\Delta M_{\text{WD}}$  in RAWD and SNBWD phases, mass lost by the donors for the three examples shown in Fig. 2. Note that these numbers do not represent the typical values in the population, which will be addressed in a subsequent paper.

Example	MS donor			HG donor			RG donor		
	BSE	IBiS	MESA	BSE	IBiS	MESA	BSE	IBiS	MESA
Duration of RAWD phase (Myr)	0.576	0.114	0.954	0.926	0.108	1.14	0.0	0.204	0.268
Duration of SNBWD phase (Myr)	0.397	0.040	0.233	0.201	0.035	0.039	0.0	0.0	0.196
$\Delta M_{\text{WD}}$ in SNBWD phase ( $M_{\odot}$ )	0.1516	0.0089	0.1068	0.049	0.0087	0.010	0.0	0.0	0.059
$\Delta M_{\text{WD}}$ in RAWD phase ( $M_{\odot}$ )	0.3088	0.0435	0.4723	0.5480	0.0417	0.5885	0.0	0.0816	0.0997
$\Delta M_{\text{d,ml}}$ of donor star ( $M_{\odot}$ )	0.8498	1.8860	0.93674	1.3264	1.8728	1.2475	0.7476	0.7515	0.7276

#### 4.1.1 The Number of SNBWD

Figures 3 and 4 show the evolution of the number of SNBWD per unit mass and their bolometric luminosity, respectively, in different models. Note immediately, that the difference is not dramatic between models with precomputed binding energy parameter  $\lambda$  and a fixed  $\alpha_{\text{ce}}$  and models with constant product  $\alpha_{\text{ce}} \times \lambda$  in the common envelope equation. This is unsurprising, given that for relatively low-mass stars  $\lambda < 1$ , and does not vary as strongly with evolutionary state as for high-mass stars (Xu & Li 2010; Loveridge, van der Sluis & Kalogera 2011).

As expected from previous studies (Yungelson 2010), the normalized number of SNBWD in case I (starburst) is larger than that for case II (constant SFR) at early age and smaller at late times. In the starburst case, the number of SNBWDs is sharply decreasing after 2 Gyr, as the reservoir of binaries with “proper” combinations of accretor and donor masses is exhausted. In the constant SFR case, SNBWDs form with a delay of about 1 Gyr relative to star formation and then “die” in about 2 Gyr, while the galaxy mass continuously increases. This is the reason for the decrease of  $(N/M_{\star})$  in the lower panel of Fig. 3. At 10 Gyr, the number of SNBWDs in BSE+MESA models may be as high



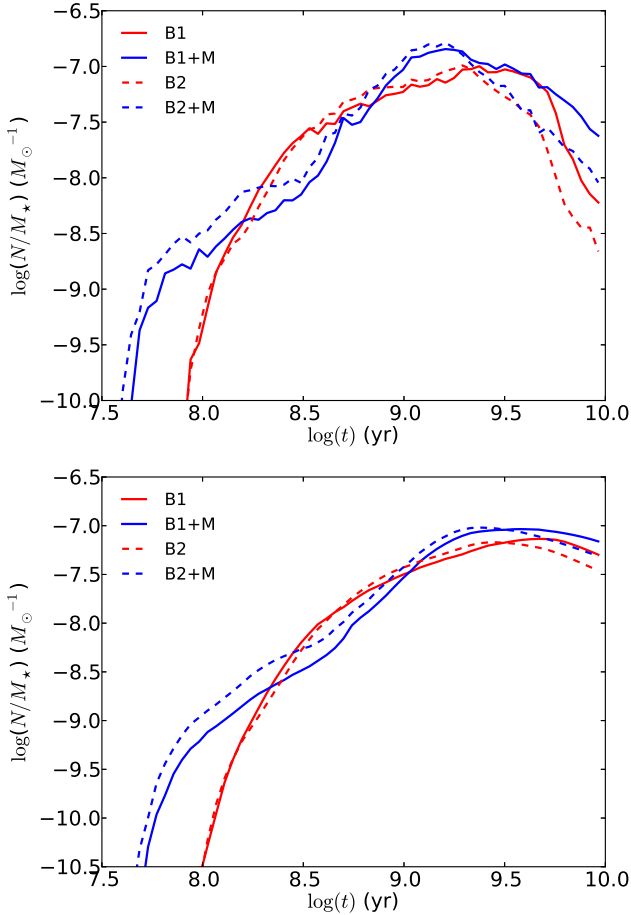


**Figure 3.** The number of SNBWDs normalised to the total stellar mass for starburst case (upper panel) and constant SFR case with  $\text{SFR} = 1 M_{\odot}/\text{yr}$  (lower panel). The blue and red lines show the results computed with BSE+MESA and BSE only, respectively.

as 4550 - 6550 in a  $10^{11} M_{\odot}$  spiral “galaxy” and 750 - 1900 in an elliptical one of the same mass. The number of SNBWDs in an elliptical galaxy at  $t = 10$  Gyr in our model is comparable to the number in the model of Yungelson (2010), while for a spiral galaxy in our model it is a little larger. Given that most of the soft X-ray emission from SNBWD is easily absorbed by interstellar gas, not all SNBWDs will be observed as SSSs. So we must emphasize that the number of SSS in the model may be estimated only after analysis of the spectra of SNBWDs (Paper II, in preparation).

If hydrogen burns steadily on the surface of a WD, its nuclear burning luminosity is

$$L_{\text{nuc}} = \epsilon_{\text{H}} X_{\text{H}} \dot{M}_{\text{acc}}, \quad (7)$$

where  $\epsilon_{\text{H}} = 6.4 \times 10^{18}$  erg/g is the nuclear energy release per unit mass of hydrogen,  $X_{\text{H}}$  is the mass fraction of hydrogen, and  $\dot{M}_{\text{acc}}$  is the accretion rate.

In Figure 4, we present the dependence of the nuclear luminosity of the SNBWDs population on time. As may be expected, it follows the evolution of the number of SNBWDs. In addition, we should note that helium burning contributes little to the total bolometric luminosity, since it is only 10% as efficient as hydrogen burning.

In Figs. 5 and 6, we show the normalized bolometric

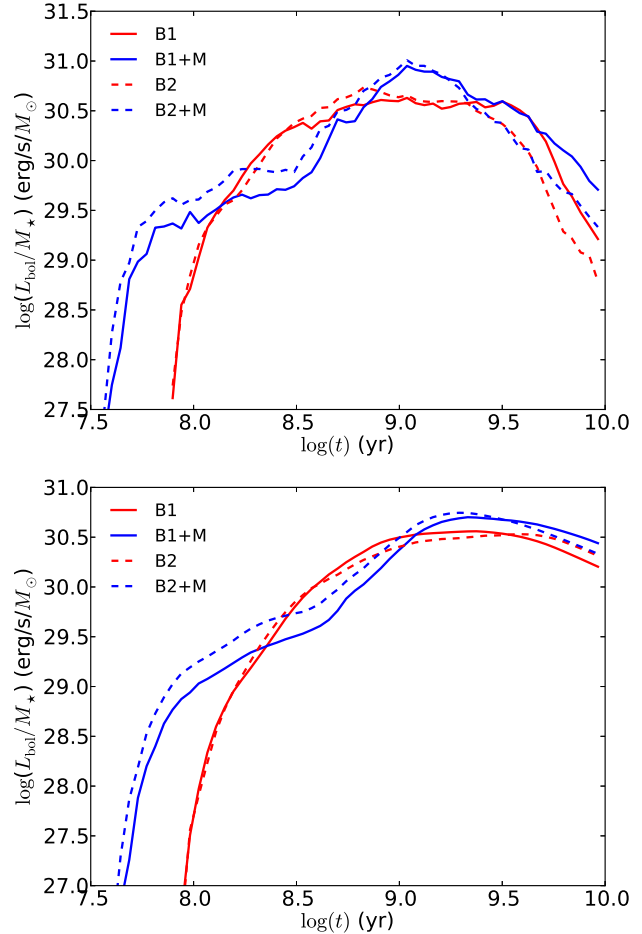


**Figure 4.** Similar to Fig. 3, but for bolometric luminosity. Upper panel — starburst case, lower panel — the case of constant SFR ( $\text{SFR} = 1 M_{\odot}/\text{yr}$ ). The blue and red lines show the results computed with BSE+MESA and BSE only, respectively.

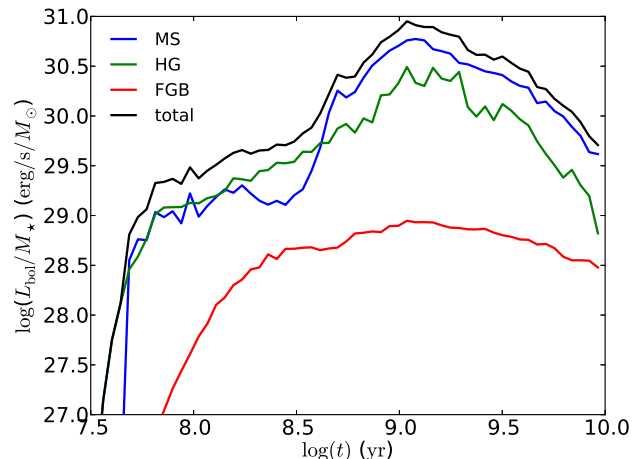


**Figure 5.** Bolometric luminosity of SNBWDs with different types of donors for starburst case in model B1+M.

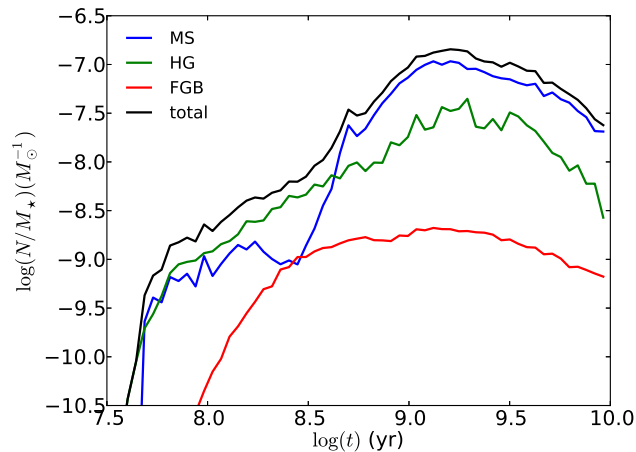


**Figure 6.** Similar to Fig. 5 but for the number of SNBWDs.

luminosity and numbers of systems with donors of different types in a starburst “galaxy”. We find that at very early times, the number of SNBWDs and their bolometric luminosity are dominated by HG systems, but after about 300 Myr (approximately the lifetime of a  $3 M_{\odot}$  star on the MS) the population becomes dominated by systems with MS-donors. Relative to MS- and HG- donor systems, those binaries which begin mass transfer on the RGB do not play a significant role at any epoch. This is due to the short time they spend in the steady hydrogen burning regime. However, in describing the number of HG donors, we should note that the donor type is defined at the onset of mass transfer. In fact, many donors which begin mass transfer on the HG reach the RGB before the end of mass transfer phase. So, this result can not be directly compared with observation.

#### 4.1.2 The Number of Rapidly Accreting WDs

The rate of mass transfer is highest at the initial stages of mass transfer and some NBWD should pass through a RAWD phase (Fig. 2). In Fig. 7, we show the evolution of the number of RAWDs in each model. It is evident that the choice in prescription for the binding parameter  $\lambda$  (whether fixed or found from an analytic fit to stellar models) does not lead to the difference in numbers exceeding  $\simeq 3$  for RAWDs.

The “delay” found between initial star formation and the formation of RAWDs is shorter in those models which use detailed calculation of post-RLOF evolution. This is a consequence of the difference in the common-envelope formation criterion: in our BSE-only models systems with massive donors are immediately rejected by the stability criterion, while in the BSE+MESA model they contribute to the number of RAWDs at very early epochs. The use of the stability criterion from Hjellming & Webbink (1987) in our BSE-only models likely results in the lower number of RAWD and NBWD compared to the BSE+MESA-based calculations.

The origin of another feature — the finite time in which RAWDs may exist in any starburst “galaxy” in models B1, B2 — may have the same reason: while BSE immediately rejects RG-donors on the base of the Hjellming & Webbink (1987) criterion for dynamically unstable mass loss, the hy-

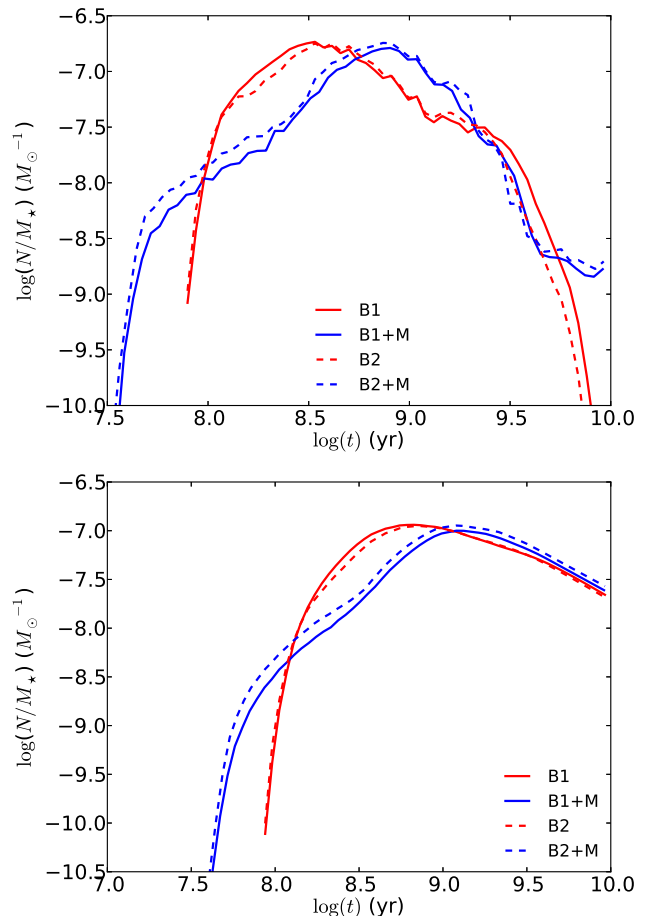


**Figure 7.** The number of RAWDs normalized to the total stellar mass at the given time for starburst case (upper panel) and constant SFR case with  $SFR = 1 M_{\odot}/yr$  (lower panel) as a function of time. The blue and red lines show the results computed with BSE+MESA and BSE only, respectively.

brid algorithm always follows the increase of  $\dot{M}$  before the formation of a CE, and RAWDs and SSSs should inevitably be present in the model, albeit with short lifetimes.

Since the existence of a RAWD phase is based on the assumption that WDs may lose mass through optically thick winds, it was suggested that they may be observable as low-luminosity Wolf-Rayet stars (possibly WR nuclei of PN?) or V Sge type cataclysmic binaries with numerous emission lines of highly ionized species in their spectra (see Lepo & van Kerkwijk 2013, and references therein). Our “spiral” model galaxies with mass  $10^{11} M_{\odot}$ , suggest the existence of 2250 - 2500 RAWDs at 10 Gyr, while in the models of early-type “galaxies” with the same mass, the number of RAWDs is 160 - 180 at 10 Gyr. RAWDs are absent at 10 Gyr in our BSE-only models, while they remain present in our models where the response of the donor is followed throughout the mass transfer phase.

This suggests that RAWDs in nearby ellipticals, such as M32, can be observed. A search for RAWDs in the central core of the Small Magellanic Cloud (Lepo & van Kerkwijk 2013) did not discover a single RAWD candidate system. Because it is still uncertain whether WD may lose mass via optically thick winds, and the appearance of RAWD has



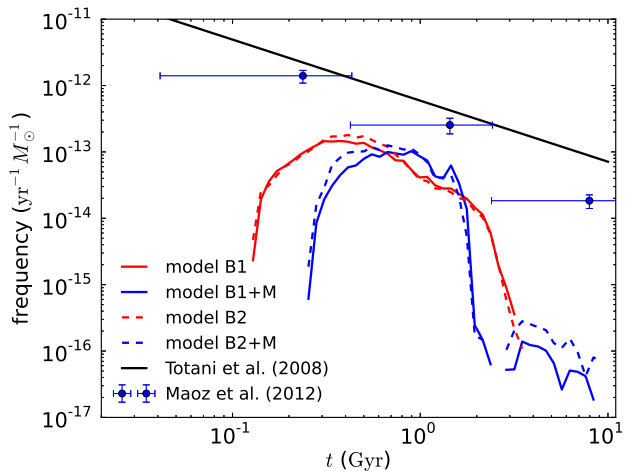


**Figure 8.** Evolution of the SNe Ia rate as a function of galaxy age for elliptical-like galaxy. The power-law line is the fitting formula from Totani et al. (2008) and the points with errorbars are the observed data from Maoz & Mannucci (2012).

never been modeled in detail, the nondetection of RAWDs does not provide constraints on the SD model of SNe Ia.

Given that accreting WDs spend a significant time as RAWDs, they can increase mass significantly and become progenitors of SNe Ia. During the RAWD phase, the WD photosphere will inflate significantly and emit predominantly in the extreme UV. Given that this EUV radiation will ionize the surrounding ISM, Woods & Gilfanov (2013, 2014) suggested that observations of emission lines, in particular in He II 4686Å, may serve to constrain the presence of high-temperature ionizing sources. In order to explore this prediction, Johansson et al. (2014) selected  $\sim 11500$  emission line galaxies and searched for a HeII emission feature. They found that it is significantly weaker than expected if the SD-scenario would be the primary channel for the production of SNe Ia. In particular, they found that the contribution of the SD-channel to the total SN Ia rate in early-type galaxies with the age  $1\text{Gyr} \leq t \leq 4\text{Gyr}$  must be  $< 5\%$ .

## 4.2 SNe Ia rates

Figure 8 shows the SNe Ia rate as a function of age for a starburst galaxy. Since the delay time distribution (DTD) is the SN rate as a function of the time elapsed between the formation of a binary and the explosion of a SN Ia, the plot also presents the DTD.

For comparison, we show the empirical DTDs found by Totani et al. (2008) and Maoz, Mannucci & Brandt (2012). From Totani et al. (2008), we have used their fit obtained assuming solar abundance and a Salpeter IMF for the stellar population. Although we have used different IMF, inspection of their table 4 reveals that the result of Totani et al. (2008) does not strongly depend on the IMF. Maoz, Mannucci & Brandt (2012) use Kroupa IMF. Similar to other studies, the SNe Ia rate produced by the SD-scenario in our models falls well below the observed one, with a DTD which does not follow the simple power-law distribution suggested by observations. It is worth noting that the peak in the DTD for our BSE+MESA models is

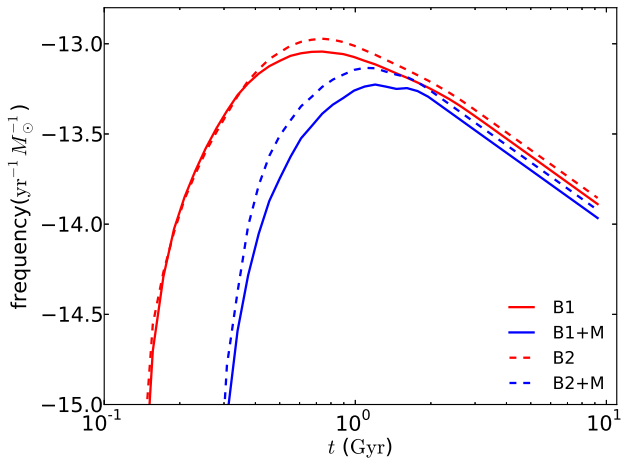


**Figure 9.** Evolution of the SNe Ia rate for spiral-like galaxy with  $\text{SFR} = 1.0 M_{\odot}/\text{yr}$ .

shifted to later times, closer to 1 Gyr, compared to the BSE models. This is mainly due to the difference in mass-transfer rate treatment, as discussed in the previous subsection.

Our peak calculated SNe Ia rate for the starburst case is still smaller than the observed rate, even though we have adopted 100% accumulation efficiency for helium burning. Figure 9 shows the SNe Ia rate for a spiral-like “galaxy” with constant  $\text{SFR} = 1.0 M_{\odot}/\text{yr}$ . Given that the current and likely for the last many Gyrs SFR in the Milky Way is  $\sim 2 M_{\odot} \text{yr}^{-1}$  (Chomiuk & Povich 2011; Kennicutt & Evans 2012)<sup>4</sup>, the SD SNe Ia rate in our simulation is  $2.0 \times 10^{-4} \text{yr}^{-1}$  at  $t = 10$  Gyr. This is  $\approx 15$ – $20$  times lower than the rate inferred for Milky Way like galaxies  $(3 - 4) \times 10^{-3}/\text{yr}$  (Cappellaro, Evans & Turatto 1999). Note that past estimates of the rate of SNe Ia from the SD-channel (e.g., Han & Podsiadlowski 2004) produced larger values partially due to a higher assumed SFR:  $3\text{--}5 M_{\odot}/\text{yr}$ .

Han & Podsiadlowski (2004); Wang, Li & Han (2010); Meng & Yang (2010) adopted a similar method to investigate the SNe Ia rate produced by WD+MS/HG binaries, but under different assumptions on SFR, binarity fraction, common envelope ejection efficiency, retention efficiency and magnetic braking. If we renormalize the rates of SNe Ia found in these papers to a SFR of  $2 M_{\odot} \text{yr}^{-1}$  and binary fraction 50%, they do not exceed  $3.6 \times 10^{-4} \text{yr}^{-1}$  which is not significantly different from the rate which we derive. Meng & Yang (2010) also investigated the effect of mass stripping and accretion-disk instability, as suggested by Hachisu et al. (2008) and King et al. (2003); these hypothetical effects may increase the rate of SNe Ia by a factor of 3-4.

In order to verify the influence of the RAWD phase on the SNe Ia rate, we also calculated the latter assuming that the WD binaries will enter CE when mass accretion rate is larger than the maximum rate for stable hydrogen burning.

<sup>4</sup> As shown by Chomiuk & Povich (2011), modern estimates of current Galactic SFR cluster around  $1.9 \pm 0.4 M_{\odot} \text{yr}^{-1}$ , if normalized to the same assumptions about the IMF of the stellar population and similar assumptions about stellar evolution are adopted (see Table 1 in the quoted paper).

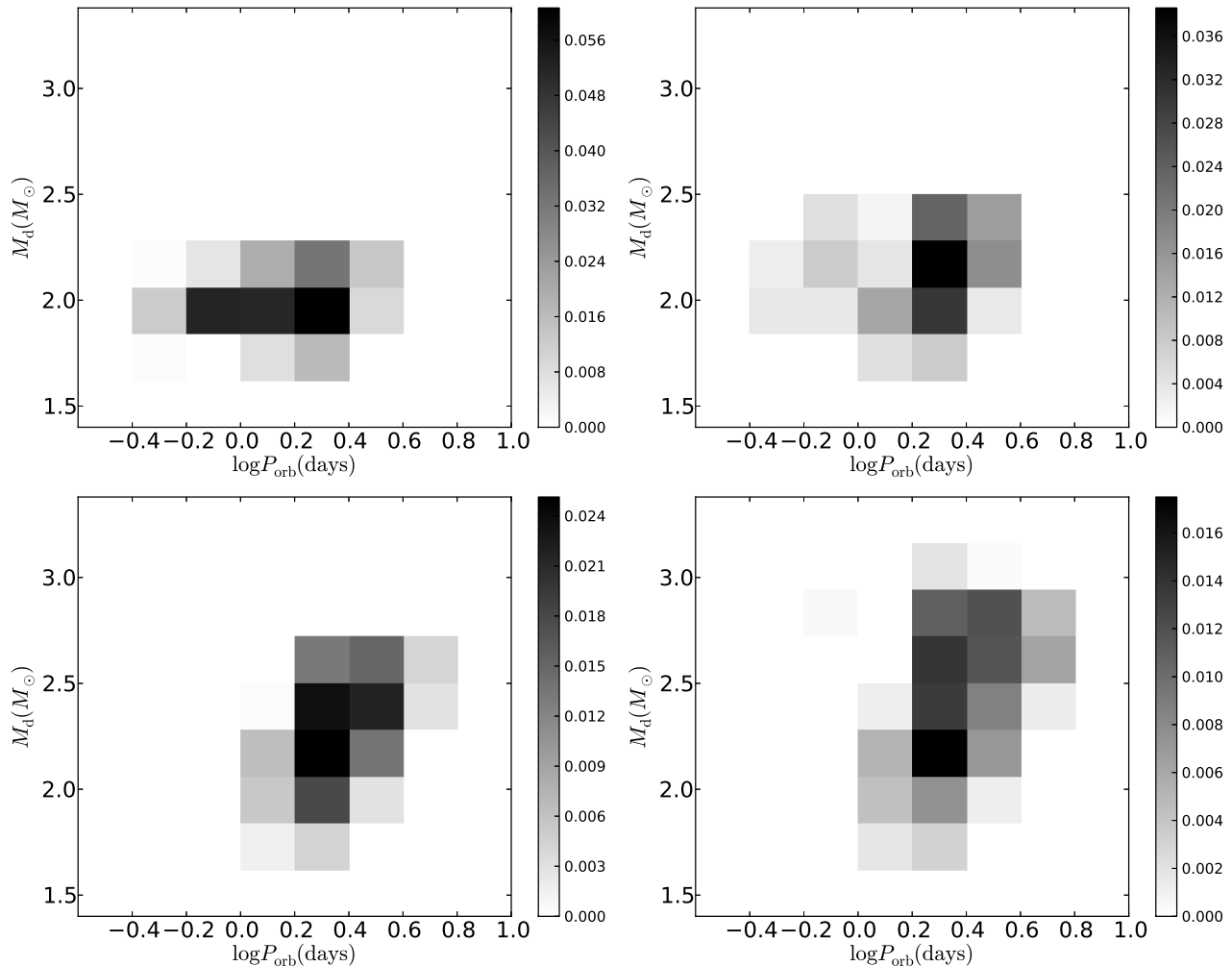


**Figure 10.** The  $P_{\text{orb}}-M_d$  distribution at the onset of mass transfer of all successful progenitors of SNe Ia for starburst case in model B1+M for different ranges of WD masses:  $0.65 \leq M_{\text{WD}} < 0.75$  (upper left panel),  $0.75 \leq M_{\text{WD}} < 0.85$  (upper right),  $0.85 \leq M_{\text{WD}} < 0.95$  (lower left) and  $0.95 \leq M_{\text{WD}} < 1.05$  (lower right). The gray scale shows the relative contribution of each pixel to the total rate of SNe Ia.

We find that SNe Ia rate becomes negligible in elliptical and spiral galaxies, in accordance with the estimates made before the introduction of optically thick winds as a stabilizing effect on mass transfer (e.g., Yungelson et al. 1996).

In Figure 10, we show the distribution of binary parameters at the onset of mass transfer for successful progenitors of SNe Ia in the starburst case. Here we only show four different WD mass ranges, since there are far fewer SNe Ia produced outside of these ranges. It is interesting to find that most of the SNe Ia come from binaries with initially less massive WDs, which is consistent with Meng, Chen & Han (2009) (see their Fig. 9). This is not difficult to understand, since most white dwarf binaries in the post-CE white dwarf binary population have relatively small-mass WDs (Han, Podsiadlowski & Eggleton 1995). Moreover, the lower mass WDs can accrete more mass in binaries with the same donor mass and orbital periods (Langer et al. 2000). Note that contribution of systems with red giant donors is insignificant in our calculation. Note, in our calculations, we do not consider possible atmospheric mass loss (Plavec et al. 1973) or enhancement of stel-

lar winds of RG close to ROLF (Podsiadlowski & Mohamed 2007), which may delay embedding of the potentially unstable system into common envelope at the instant of RLOF (e.g. Podsiadlowski & Mohamed 2007).

### 4.3 Uncertainty of common envelope evolution

It is widely understood that the outcome of CE evolution suffers from many uncertainties, such as the available sources of energy (e.g. Ivanova et al. 2013; Zorotovic et al. 2014). In our calculation, we adopt  $\alpha = 0.25$  and a fitting formula for  $\lambda$ . In the fitting formula for  $\lambda$ , the internal energy such as thermal energy of the gas and radiation energy are included (see Eq. (1) in Loveridge, van der Sluys & Kalogera 2011). Given the uncertainty of CE evolution, we performed a set of calculations of the model B1 increasing  $\alpha$  to 1. In Fig. 11, we compare the evolution of SNBWDs and SNe Ia rate in the starburst case for  $\alpha = 0.25$  and  $\alpha = 1.0$ . We found that there is no dramatic difference between  $\alpha = 1.0$  and  $\alpha = 0.25$ . For  $\alpha = 1.0$ , SNBWD, as well as SN Ia events appear slightly later than for  $\alpha = 0.25$ , since after the first

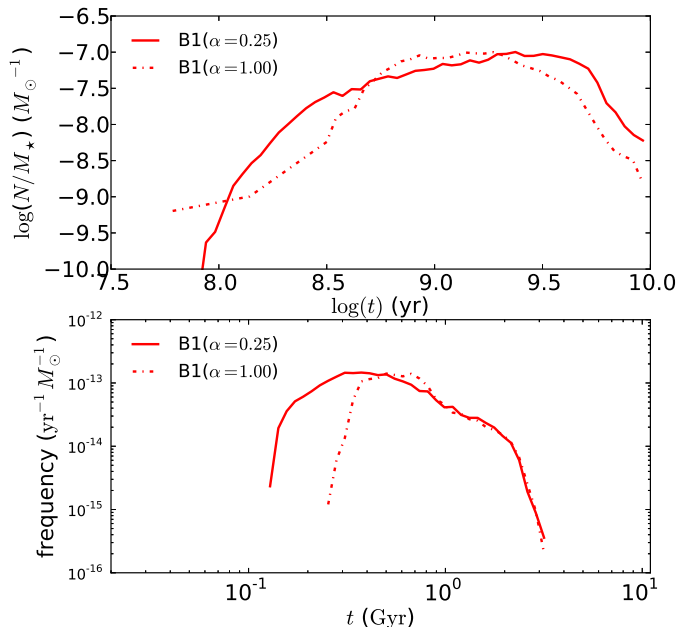


**Figure 11.** Comparison of mass-normalized SNBWDs number (upper panel) and SNe Ia rate (lower panel) for starburst case in the default configuration (solid line) and assuming  $\alpha = 1.0$  (dash-dotted line).

common envelope episode systems are wider. A similar effect was noted before by Wang, Li & Han (2010). We also found no significant difference for RAWDs, which are not shown here.

#### 4.4 Remarks about the noise in population synthesis calculations

In the above plots, especially Fig. 5, 6 and 8, one may note that the curves are noisy. This problem is commonly seen in population synthesis studies. There are several reasons for that, both in our BSE-only calculation as well as in our BSE+MESA calculation, the primary causes being:

- In our BSE-only calculation, one cause for the noise is that we have adopted several different CE criteria for different binaries. This is especially important for those binaries that begin mass transfer on the HG, which evolve to the RG phase prior to the end of the mass transfer phase. Typically, our HG-donor tracks end abruptly when they violate the stability condition of Hjellming & Webbink (1987). However, just prior to this, many tracks “dip back” into the stable burning regime. Whether this occurs or not does not depend smoothly on the time of onset of mass transfer, therefore introducing small variations in the numbers and luminosity of SNBWDs predicted in our calculations.

- In addition to this, the limited number of tracks in the calculation will also contribute to the noise. In particular, in our BSE+MESA calculations, we perform a mapping from a set of  $\sim 100,000$  tracks produced by BSE, to one of  $\sim 30,000$  tracks produced by MESA. The discontinuous transition from our BSE grid to a much coarse grid of MESA tracks introduces unphysical variability in our output.

- Finally, the noise in the Fig. 8 is primarily due to the small number of binary tracks which explode as SNe Ia.

## 5 SUMMARY AND CONCLUSIONS

In this work, we combined the population synthesis code BSE with the detailed stellar evolutionary code MESA for the first time, in order to study the population of accreting WDs. We also compared the output from this with the results obtained applying a “rapid” algorithm, using BSE alone. With these two BPS algorithms, we investigated the evolution of the number of rapidly accreting white dwarfs, stable nuclear burning white dwarfs and the SNe Ia rate in elliptical and spiral-like galaxies. In addition to confirming that the SD channel is subdominant in producing the overall SN Ia rate, we also evaluated the effect of implementing differing treatments of mass transfer for the results of BPS calculations.

Comparing the two versions of our binary population synthesis calculations, we found that the mass transfer prescription in BPS is especially important for calculating the number and total luminosity of nuclear-burning white dwarfs in elliptical galaxies at early and late epochs (from initial starburst). We argue that this also partially explains the differences in SNe Ia rates and DTD obtained by different binary population synthesis groups. We found that RAWDs appear earlier in our BSE+MESA model compared with BSE-only, due to the accreting WDs with massive donors found in the former.

We find that there is a factor of  $\approx 3$  difference between the results of our calculations using a fitting formula for the binding parameter  $\lambda$  (Loveridge, van der Sluys & Kalogera 2011) and a constant  $\alpha_{ce} = 0.25$ , and our calculations using a constant  $\alpha_{ce} \times \lambda = 0.25$ .

In our BSE+MESA model, we found that the number of RAWDs at 10 Gyr is 160 – 180 for an elliptical galaxy of  $10^{11} M_{\odot}$  and 2250 – 2500 for a spiral-like galaxy of the same mass. This result is in stark contrast with zero RAWDs predicted in our calculation for a model elliptical galaxy using BSE alone.

We find that the number of SNBWD is 750 – 1900 in our model elliptical-like galaxy and 4550 – 6550 in our model spiral-like galaxy (both with  $M = 10^{11} M_{\odot}$  at 10 Gyr).

The predicted SD SNe Ia rate for a Milky-Way-like galaxy is found to be  $\simeq 2.0 \times 10^{-4} \text{yr}^{-1}$ , more than an order of magnitude lower than the observationally inferred total Galactic SNe Ia rate. Our DTD for the SD-model is inconsistent with the observed DTD  $\propto t^{-1}$ . If we assume that RAWDs do not exist, but rather that a common envelope is formed if the accretion rate onto a WD is larger than the upper limit for stable hydrogen burning, then the rate of SNe Ia produced by the SD-channel becomes negligible.

To conclude our discussion of the significance of the SD-channel for the production of SNe Ia, we note the following. Since WDs in the steady burning phase can effectively accumulate mass, it is widely suggested that SSSs be identified with the progenitors of SNe Ia and, therefore, observations of SSSs may be useful for constraining the SD model. Gilfanov & Bogdán (2010) estimated the expected X-ray flux from the progenitors of SNe Ia in the SD-scenario for elliptical galaxies based on the observed supernova rate.

They found that the observed X-ray flux from six nearby elliptical galaxies is 30 – 50 times smaller than the predicted value, and constrain the contribution of the SD-channel to < 5%. In a similar way, Di Stefano (2010) found that there are too few SSSs to account for the SNe Ia rate. Even if accreting WDs radiate at significantly lower temperatures ( $T \approx 10^5 K$ ), due to the inflation of their photospheres, the SD channel may still be limited to providing < 10% of the SNe Ia rate (Woods & Gilfanov 2013; Johansson et al. 2014).

Yungelson et al. (1996), Di Stefano (2010), and Yungelson (2010) considered the possibility that some SSSs may reside in wind-accreting systems which later produce double-degenerate systems (symbiotic stars), and estimated their number in the Galaxy as  $\sim 10^3$ , while the estimate by Nielsen et al. (2014) is even lower:  $\sim 10^2$ . Though several  $10^3$  SNBWDs in the model is apparently a large number, it is still about 2 orders of magnitude lower than that necessary to be consistent with the observationally inferred Galactic SNe Ia rate. Lü et al. (2006) and Nielsen et al. (2014) estimated that in wind-fed systems WD typically accrete no more than  $\approx 0.1M_{\odot}$ .

## ACKNOWLEDGMENTS

We would like to thank an anonymous referee for useful comments, which helped to improve the paper. HLC gratefully acknowledges support and hospitality from the MPG-CAS Joint Doctoral Promotion Program (DPP) and Max Planck Institute for Astrophysics (MPA). This work of HLC and ZWH was partially supported by the National Natural Science Foundation of China (Grant Nos. 11033008, 11390374). The work is also partially supported by Presidium of the Russian Academy of Sciences P-21 and RFBR grant 14-02-00604. LRY gratefully acknowledges warm hospitality and support from MPA-Garching. MG acknowledges hospitality of the Kazan Federal University (KFU) and support by the Russian Government Program of Competitive Growth of KFU. HLC acknowledges the computing time granted by the Yunnan Observatories and provided on the facilities at the Yunnan Observatories Supercomputing Platform.

## REFERENCES

- Abt H. A., 1983, *ARA&A*, 21, 343  
 Bloom J. S. et al., 2012, *ApJL*, 744, L17  
 Bours M. C. P., Toonen S., Nelemans G., 2013, *A&A*, 552, A24  
 Cappellaro E., Evans R., Turatto M., 1999, *A&A*, 351, 459  
 Chomiuk L., Povich M. S., 2011, *AJ*, 142, 197  
 Davis P. J., Kolb U., Willems B., 2010, *MNRAS*, 403, 179  
 de Kool M., 1990, *ApJ*, 358, 189  
 Dewi J. D. M., Tauris T. M., 2000, *A&A*, 360, 1043  
 Di Stefano, R. 2010, *ApJ*, 719, 474  
 Duquennoy A., Mayor M., 1991, *Astron. Astrophys.*, 248, 485  
 Gilfanov M., Bogdán Á., 2010, *Nature*, 463, 924  
 Hachisu I., Kato M., Nomoto K., 1999, *ApJ*, 522, 487  
 Hachisu, I., Kato, M., & Nomoto, K. 2008, *ApJ*, 679, 1390  
 Han Z., Podsiadlowski P., 2004, *MNRAS*, 350, 1301  
 Han Z., Podsiadlowski P., Eggleton P. P., 1995, *MNRAS*, 272, 800  
 Hillebrandt W., Kromer M., Röpke F. K., Ruiter A. J., 2013, *Frontiers of Physics*, 8, 116  
 Hjellming M. S., Webbink R. F., 1987, *ApJ*, 318, 794  
 Hurley J. R., Tout C. A., Pols O. R., 2002, *MNRAS*, 329, 897 their  
 Iben, Jr. I., Tutukov A. V., 1984, *ApJS*, 54, 335  
 Iben, Jr. I., Tutukov A. V., 1989, *ApJ*, 342, 430  
 Idan I., Shaviv N. J., Shaviv G., 2013, *MNRAS*, 433, 2884  
 Ivanova N. et al., 2013, *Astron. Astrophys. Rev.*, 21, 59  
 Ivanova N., Taam R. E., 2004, *ApJ*, 601, 1058  
 Johansson J., Woods T. E., Gilfanov M., Sarzi M., Chen Y.-M., Oh K., 2014, *ArXiv e-prints*  
 Kennicutt R. C., Evans N. J., 2012, *ARA&A*, 50, 531  
 Kraicheva Z. T., Popova E. I., Tutukov A. V., Yungelson L. R., 1979, *SvA*, 23, 290  
 King, A. R., Rolfe, D. J., & Schenker, K. 2003, *MNRAS*, 341, L35  
 Kroupa P., 2001, *MNRAS*, 322, 231  
 Langer N., Deutschmann A., Wellstein S., Höflich P., 2000, *A&A*, 362, 1046  
 Lepo K., van Kerkwijk M., 2013, *ApJ*, 771, 13  
 Lin J., Rappaport S., Podsiadlowski P., Nelson L., Paxton B., Todorov P., 2011, *ApJ*, 732, 70  
 Loveridge A. J., van der Sluys M. V., Kalogera V., 2011, *ApJ*, 743, 49  
 Lü, G., Yungelson, L., & Han, Z. 2006, *MNRAS*, 372, 1389  
 Madhusudhan, N., Rappaport, S., Podsiadlowski, P., & Nelson, L. 2008, *ApJ*, 688, 1235  
 Maoz D., Mannucci F., 2012, *PASA*, 29, 447  
 Maoz D., Mannucci F., Brandt T. D., 2012, *MNRAS*, 426, 3282  
 Maoz D., Mannucci F., Nelemans G., 2013, *ArXiv e-prints*  
 Matteucci F., Greggio L., 1986, *A&A*, 154, 279  
 Meng, X., & Yang, W. 2010, *ApJ*, 710, 1310  
 Meng X., Chen X., Han Z., 2009, *MNRAS*, 395, 2103  
 Morton D. C., 1960, *ApJ*, 132, 146  
 Nelson L., 2012, *Journal of Physics Conference Series*, 341, 012008  
 Newsham, G., Starrfield, S., & Timmes, F. 2013, *arXiv:1303.3642*  
 Nielsen, M. T. B., Nelemans, G., Voss, R., & Toonen, S. 2014, *A&A*, 563, A16  
 Nugent P. E. et al., 2011, *Nature*, 480, 344  
 Paczyński, B. 1971, *Acta. Astron.*, 21, 417  
 Paczyński B., Ziółkowski J., Zytkow A., 1969, in *Mass Loss from Stars*, p. 237  
 Paczyński B., Sienkiewicz R., 1972, *Acta. Astron.*, 21, 1  
 Passy J.-C., Herwig F., Paxton B., 2012, *ApJ*, 760, 90  
 Paxton B., Bildsten L., Dotter A., Herwig F., Lesaffre P., Timmes F., 2011, *ApJS*, 192, 3  
 Paxton B. et al., 2013, *ApJS*, 208, 4  
 Perlmutter S. et al., 1999, *ApJ*, 517, 565  
 Podsiadlowski, P., Rappaport, S., & Pfahl, E. D. 2002, *ApJ*, 565, 1107  
 Pfahl, E., Rappaport, S., & Podsiadlowski, P. 2003, *ApJ*, 597, 1036  
 Paczynski, B., & Zytkow, A. N. 1978, *ApJ*, 222, 604  
 Plavec, M., Ulrich, R. K., & Polidan, R. S. 1973, *PASP*, 85, 769

- Podsiadlowski, P., & Mohamed, S. 2007, *Baltic Astronomy*, 16, 26
- Prialnik D., Kovetz A., 1995, *ApJ*, 445, 789
- Rappaport S., Verbunt F., Joss P. C., 1983, *ApJ*, 275, 713
- Ricker P. M., Taam R. E., 2012, *ApJ*, 746, 74
- Riess A. G. et al., 1998, *AJ*, 116, 1009
- Ritter, H. 1988, *A&A*, 202, 93
- Ruiter A. J., Belczynski K., Fryer C., 2009, *ApJ*, 699, 2026
- Toonen, S., Claeys, J. S. W., Mennekens, N., & Ruiter, A. J. 2014, *A&A*, 562, A14
- Totani T., Morokuma T., Oda T., Doi M., Yasuda N., 2008, *PASJ*, 60, 1327
- Tutukov A. V., Yungelson L. R., 1981, *Nauchnye Informatsii*, 49, 3
- Wang B., Li X.-D., Han Z.-W., 2010, *MNRAS*, 401, 2729
- Webbink R. F., 1984, *ApJ*, 277, 355
- Whelan J., Iben, Jr. I., 1973, *ApJ*, 186, 1007
- Willems, B., & Kolb, U. 2004, *A&A*, 419, 1057
- Wolf, W. M., Bildsten, L., Brooks, J., & Paxton, B. 2013, *ApJ*, 777, 136
- Woods, T. E., & Gilfanov, M. 2013, *MNRAS*, 432, 1640
- Woods, T. E., & Gilfanov, M. 2014, *MNRAS*, 350
- Woods T. E., Ivanova N., 2011, *ApJL*, 739, L48
- Xu, X.-J., & Li, X.-D. 2010, *ApJ*, 716, 114
- Yaron O., Prialnik D., Shara M. M., Kovetz A., 2005, *ApJ*, 623, 398
- Yungelson L., Livio M., Truran J. W., Tutukov A., Fedorova A., 1996, *ApJ*, 466, 890
- Yungelson L., Livio M., Tutukov A., Kenyon S. J., 1995, *ApJ*, 447, 656
- Yungelson, L., & Livio, M. 1998, *ApJ*, 497, 168
- Yungelson L. R., 2010, *Astronomy Letters*, 36, 780
- Zorotovic M., Schreiber M. R., Gänsicke B. T., Nebot Gómez-Morán A., 2010, *A&A*, 520, A86
- Zorotovic, M., Schreiber, M. R., & Parsons, S. G. 2014, *A&A*, 568, L9